Technical Memorandum

To: Jeff Uhlmeyer

From: Lauren Gardner, Gonzalo Rada, and Kevin Senn

cc: Mustafa Mohamedali

Date: October 1, 2020

Re. Forensic Desktop Study Report: Maryland LTPP Test Section 24_1634

The Long-Term Pavement Performance GPS-2 Asphalt Concrete on Bound Base test section 24_1634[1] was nominated for a desktop study under TPF-5(332) "LTPP Forensic Evaluations." The test section was incorporated into the LTPP program in 1988 and was moved to the GPS-6C AC Overlay Using Modified Asphalt of AC Pavement-No Milling study in May of 1998 after receiving a shoulder restoration and 3.2-inch AC overlay. Additionally, the site was also included in the LTPP Seasonal Monitoring Program (SMP) between 1994 and 1998. As part of the SMP, the section was instrumented with an on-site weather station, along with subsurface temperature, moisture, frost detection, and water table depth sensors. The collection of FWD measurements and the downloading of the climatic information were performed monthly, and data collection of profile measurements were conducted quarterly. As a test section with particularly rich data, an investigation and comparison of the performance of the pavement prior to and following the AC overlay was conducted. This desktop study examines 1) the reason(s) for high amounts of fatigue and NWP longitudinal cracking following the AC overlay of the test section, 2) the reason(s) for the extremely low IRI on the pavement section despite the presence of cracking throughout time, and 3) the relationship between the pavement deflection, pavement temperature, and subgrade moisture content using the SMP dataset.

SITE DESCRIPTIONS

LTPP test section 24_1634 was located on State Route 90, eastbound, in Worcester County, Maryland. State Route 90 is a rural principal arterial with one lane in the direction of traffic. The test section was classified as being in a Wet, No-Freeze climate zone. The coordinates (in degrees) of the site were 38.37158, -75.25976. Photograph 1 shows the section at Station 0+00 looking eastbound in 2016, while Map 1 shows the geographical location of the test section.

[1] First two digits in test section number represent the State Code [24 =Maryland]. The final four digits are unique within each State/Province and were assigned at the time the test section was accepted into the LTPP program.

Wood Environment & Infrastructure Solutions, Inc.
12000 Indian Creek Ct, Suite F
Beltsville, MD 20705
+1 301-210-5105
www.woodplc.com

Photograph 1. LTPP Section 24_1634 at Station 0+00 looking eastbound in 2016.

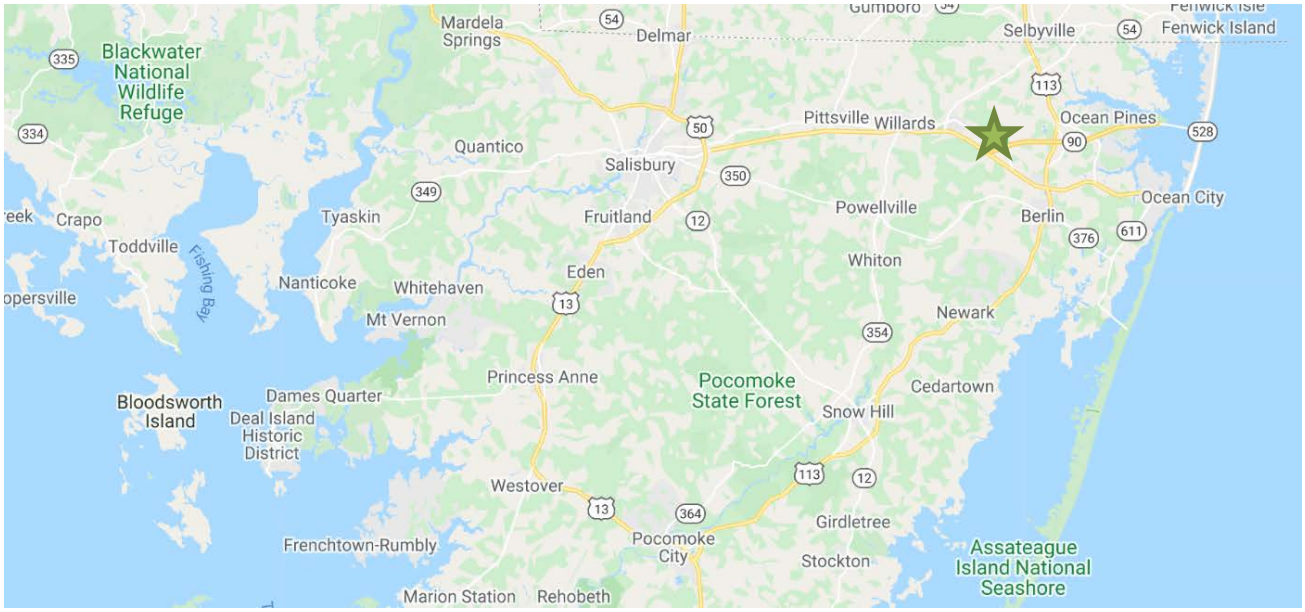

Map 1. Geographical location of test section.

BASELINE PAVEMENT HISTORY

This section of the document presents historical data on the pavement structure and its structural capacity, climate, traffic, and pavement distresses.

Pavement Structure and Construction History

The test section was constructed in 1976 and was accepted into the LTPP Program as part of the GPS-2 experiment in November 1988. The pavement structure at the time of its incorporation into the LTPP program consisted of 3.5 inches of asphalt concrete (AC), 4.8 inches of bound (sand asphalt) treated base, and 13 inches of unbound granular subbase over a fine-grained subgrade layer. This pavement structure is summarized in Table 1 and corresponds to CONSTRUCTION_NO = 1 (CN = 1) in the LTPP database. The next construction event occurred in May 1998, when the test section received shoulder restoration and a 3.2-inch AC overlay. Subsequently, the test section was moved to the GPS-6C AC Overlay Using Modified Asphalt of AC Pavement-No Milling study. Table 2 summarizes the pavement structure following the overlay which corresponds to CONSTRUCTION_NO = 2 (CN = 2). While no additional construction events were reported following 1998, the test section was found to be milled and overlaid sometime after the last survey date in 2016 (the specific year of the event is still being determined), and therefore, the site is now considered Out of Study (OOS).

Table 1. Pavement structure for 24_1634 (CN=1)

Layer Number	Layer Type	Thickness (in.)	Material Code Description
1	Subgrade (untreated)		Fine-Grained Soil: Silt
2	Unbound (granular) subbase	13	Soil-Aggregate Mixture (Predominantly Coarse-Grained)
3	Unbound (granular) subbase	4	Fine-grained Soils
4	Bound (treated) base	4.8	Sand Asphalt
5	Asphalt Concrete (AC)	3.5	Hot Mixed, Hot Laid Asphalt Concrete (AC), Dense Graded

Table 2. Pavement structure for 24_1634 (CN=2)

Layer Number	Layer Type	Thickness (in.)	Material Code Description
1	Subgrade (untreated)		Fine-Grained Soil: Silt
2	Unbound (granular) subbase	13	Soil-Aggregate Mixture (Predominantly Coarse-Grained)
3	Unbound (granular) subbase	4	Fine-grained Soils
4	Bound (treated) base	4.8	Sand Asphalt
5	Asphalt Concrete (AC)	3.5	Hot Mixed, Hot Laid Asphalt Concrete (AC), Dense Graded
6	Asphalt Concrete (AC)	1.7	Recycled AC, Hot Laid, Central Plant Mix
7	Asphalt Concrete (AC)	1.5	Hot Mixed, Hot Laid AC, Dense Graded

Pavement Structural Properties

Figure 1 and Figure 2 show the average Falling Weight Deflectometer (FWD) deflections under the nominal 9,000-pound load plate during the entire period the test section has been in study (Figure 1) and during the SMP analysis period (Figure 2). The deflection of the sensor located in the center of the load plate is a general indication of the total "strength" or response of all layers in the pavement structure to a vertically applied load. Similarly, Figure 3 shows the average deflection 48 inches from the load plate during the SMP analysis period. Because of how the FWD (or other) load is distributed on an AC pavement, deflections at 48 inches are due almost in their entirety to the subgrade response (i.e., no influence from AC and base layers). As shown in the Figure 2 and Figure 3, the deflections observed can be influenced by pavement temperature at the time of testing and moisture conditions. The gravimetric moisture content shown in both figures was calculated from Time Domain Reflectometry (TDR) sensor data collected at a depth of 26 inches below the surface of the pavement, i.e., at the top of the subgrade. The pavement temperature depicted in the figures represents the average pavement temperature at the time of testing 0.98 inches below the surface (measured during FWD testing), or within the AC layer.

As depicted in Figure 2, the change in deflection under the load plate over time appears to be directly related to the change in pavement temperature over time. For the most part, increases and decreases in deflections correspond to increases and decreases in the pavement temperature. Exceptions include the decrease in the average deflection observed in May 1996 and the decrease in average deflection in October 1996 despite an increase in pavement temperature for those two months. The relationship between the average deflection and moisture content of the test section is less clear under the center load plate. It is generally expected that as the moisture content and pavement temperature increase, deflections will also increase, but this does not appear to be the case for the gravimetric moisture content.

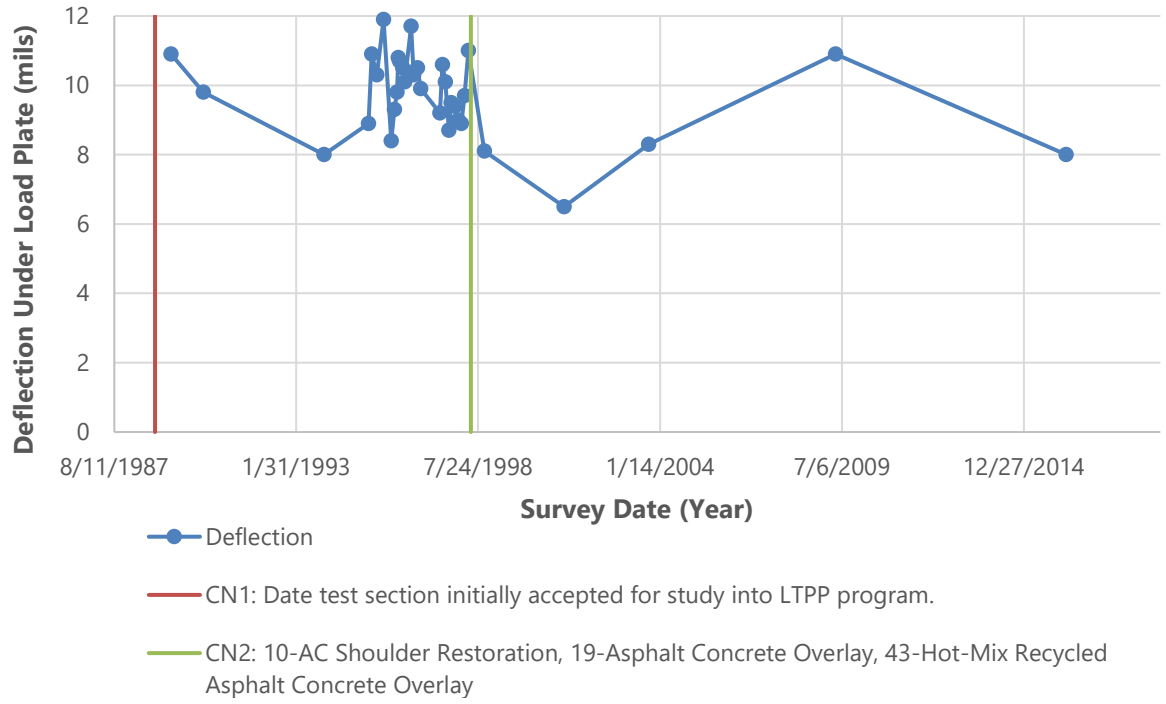

Figure 1. FWD deflections under the load plate over time.

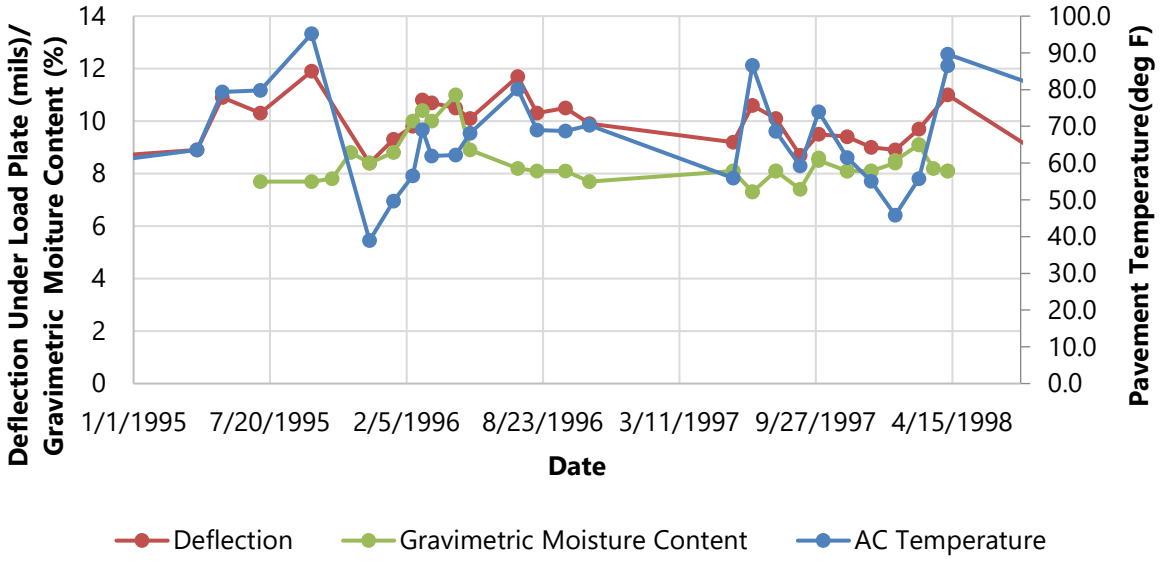

Figure 2. Comparison of a) FWD deflections under the load plate (Sensor 1), b) the average temperature of the pavement taken at a depth of 0.98 inches below the surface, and c) the gravimetric moisture content at a depth of 26 inches below the surface of the pavement (TDR 3).

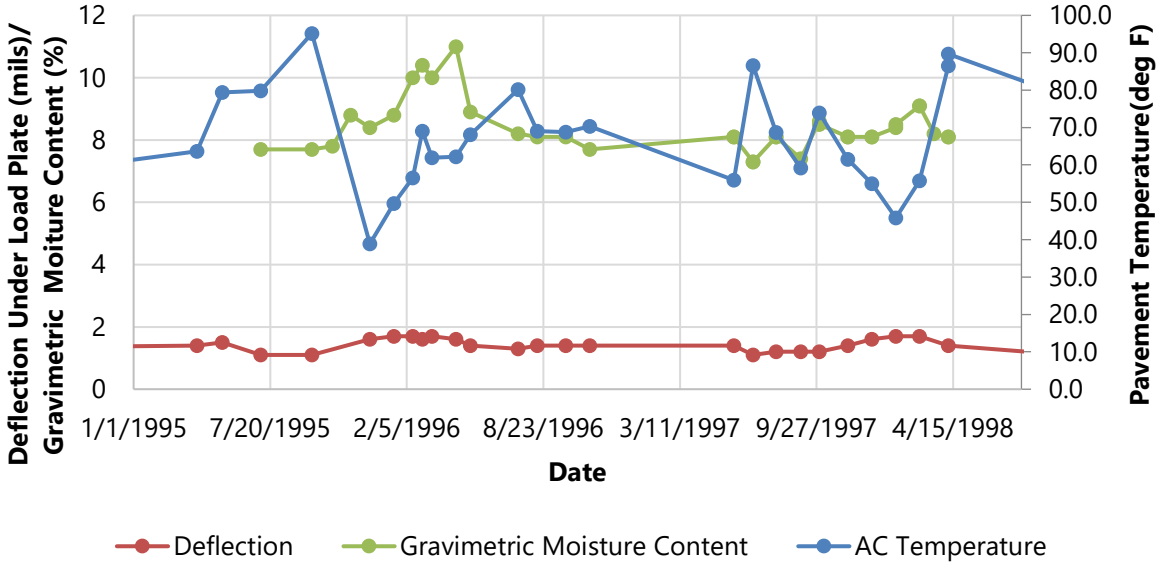

Figure 3. Comparison of a) FWD deflections 48" from the load plate (Sensor 7), b) the average temperature of the pavement taken at a depth of 0.98 inches below the surface, and c) the gravimetric moisture content at a depth of 26 inches below the surface of the pavement (TDR 3).

In Figure 3, the opposite seems to be the case—the change in deflection 48 inches from the load plate (Sensor 7) appears to be related to the change in moisture content over time, but not to the change in temperature over time. For the most part, as the moisture content increases, the average deflections increase, and as the moisture content decreases, the average deflections also decrease. The relationship between deflection and temperature is less clear; as shown in the figure, it appears that the pavement deflection increases as the temperature decreases and vice versa.

The layer moduli backcalculated from the deflection data were also assessed for the test section. The pavement structure for test section 24_1634 was modeled as 3.6 inches of AC and 4.8 inches of AC treated base over subgrade (divided into two layers). Following CN=2 in 1998, the pavement structure for the test section was modeled as 6.8 inches of AC and 4.8 inches of AC treated base over subgrade (divided into two layers). The backcalculated moduli for each layer between April 1989 and April 2009 (32 dates in total) are shown in Figure 4 to Figure 7. The collection of FWD data in 2016 was not completed until after the completion of LTPP contract to backcalculate moduli data, and therefore the backcalculated modui were not included in the LTPP database.

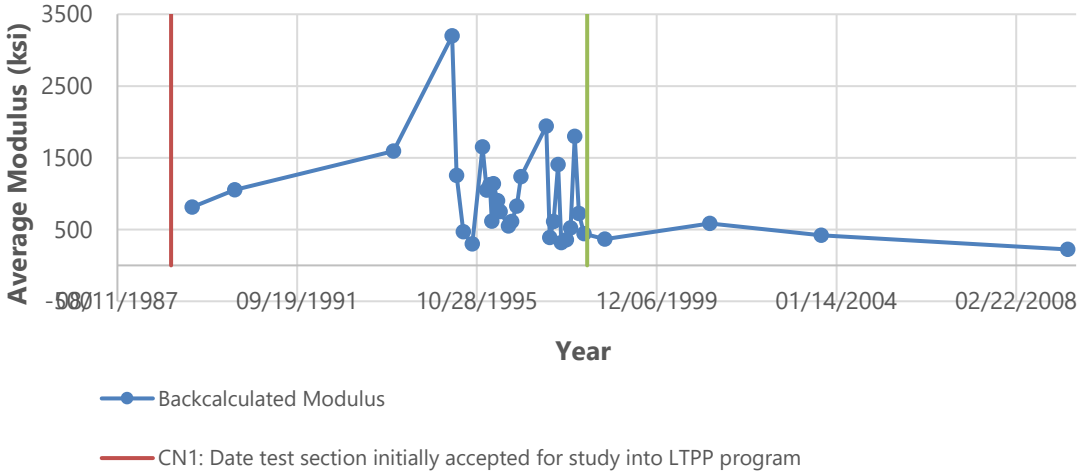

Figure 4. Average backcalculated modulus for AC (Layer 1).

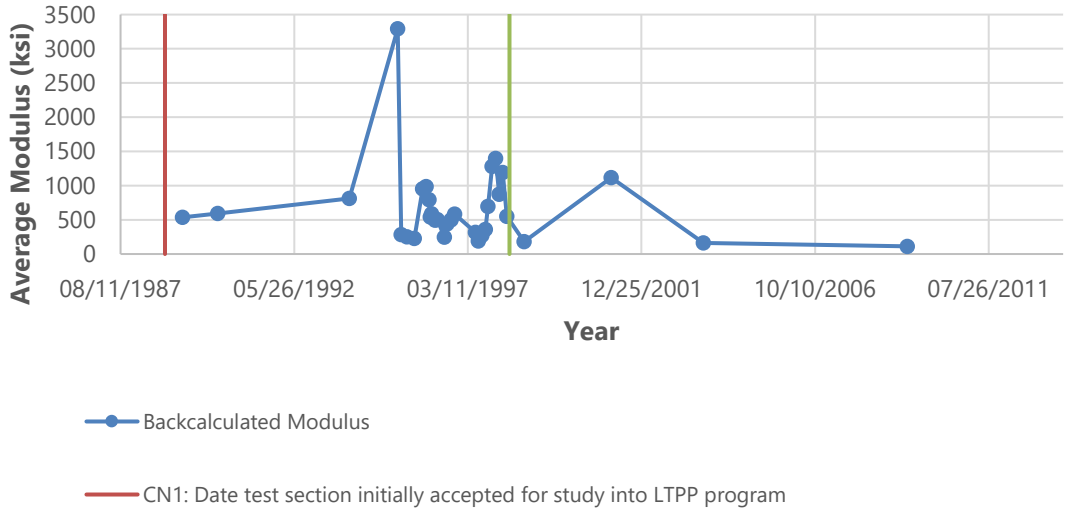

Figure 5. Average backcalculated modulus for AC treated base (Layer 2).

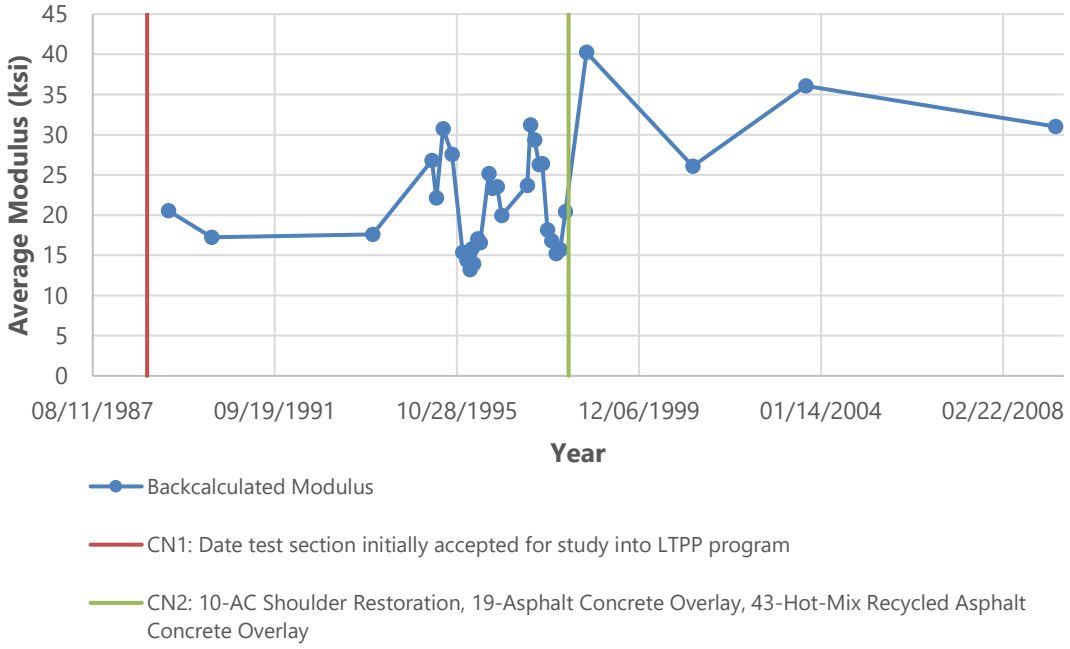

Figure 4. Average backcalculated modulus for top 24 inches of subgrade (Layer 3).

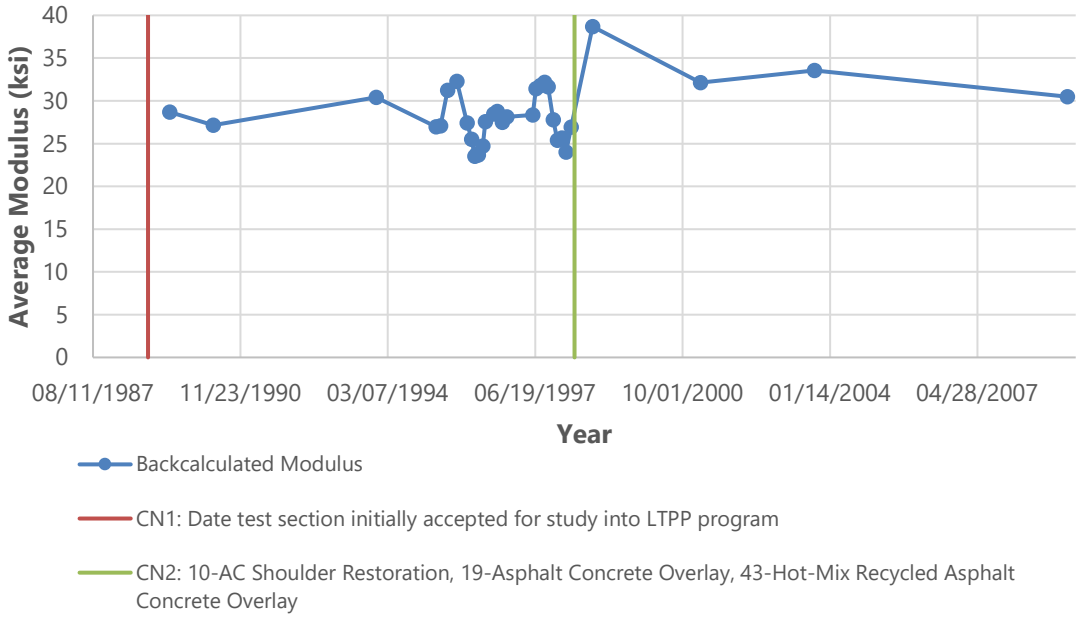

Figure 5. Average backcalculated modulus for subgrade (Layer 4).

For the most part, the moduli values calculated for each layer appear to be reasonable. Some exceptions include the moduli values reported for the AC layer and AC treated base in April of 1995. These moduli values, which reach over 3,000 ksi, appear to be outliers and not representative of the actual moduli values of these two layers. In addition to the outlier values, following the overlay in 1998, there seems to be compensating layer effects occurring between the subgrade layers and base and AC layers. The compensating layer effect is the result of the way the modulus of each layer is calculated, from the subgrade upward. While the values of the subgrade moduli appear to be reasonable, the values collected

in subsequent layers (i.e., base and asphalt layers) result in calculated values that over or underestimate the modulus as the model aims to compensate for errors incurred through the iterative backcalculation process. Therefore, following the 1998 overlay, when the moduli values of the subgrade layers decrease, the base and AC layer moduli increase and vice versa.

The reasonableness of the backcalculated layer moduli was compared to moduli derived from laboratory resilient modulus testing. Table 3 summarizes the laboratory test results for the AC, subbase, and subgrade layers; testing results were not reported for the AC treated base. For the AC layer, moduli values are shown for three test temperatures – 41, 77 and 104°F, respectively. As shown in Figure 8, the AC modulus versus temperature relationship for the field- and lab-derived resilient moduli appears to be reasonable; while there is some scatter due to the variation in backcalculated moduli results, there appears to be a clear trend between temperature and the AC layer modulus. For the unbound granular subbase and subgrade layers (which correspond to Layers 3 and 4 of the backcalculated moduli), various statistical analyses were conducted for the range of stress states (confining and deviatoric stresses) to which the laboratory samples were subjected. While the range of values in the subbase were similar to the backcalculated values reported for Layer 3, the laboratory values for the subgrade were slightly lower than the backcalcuated moduli reported for Layer 4. However, overall, the values appeared reasonable given the pavement structure.

Table 3. Laboratory Resilient Modulus Test Results

Layer	Temperature (°F)	Number of Samples/test results	Range of moduli values (ksi)	Range of Confining Stress (psi)	Range of Maximum Nominal Axial Stress (psi)
AC	41	1 sample (2 tests, original AC layer and AC overlay)	1,843-2,941	N/A	N/A
	77	1 sample (2 tests, original AC layer and AC overlay)	329-925	N/A	N/A
	104	1 sample (2 tests, original AC layer and AC overlay)	109-244	N/A	N/A
Treated Base	N/A	N/A	N/A	N/A	N/A
Subbase	N/A	1 sample (15 test results each)	17.8 to 39.3 (Average of 27.9)	3 to 20	3 to 40
Subgrade	N/A	1 sample (15 test results each)	9 to 15.7 (Average of 12.4)	2 to 6	2 to 10

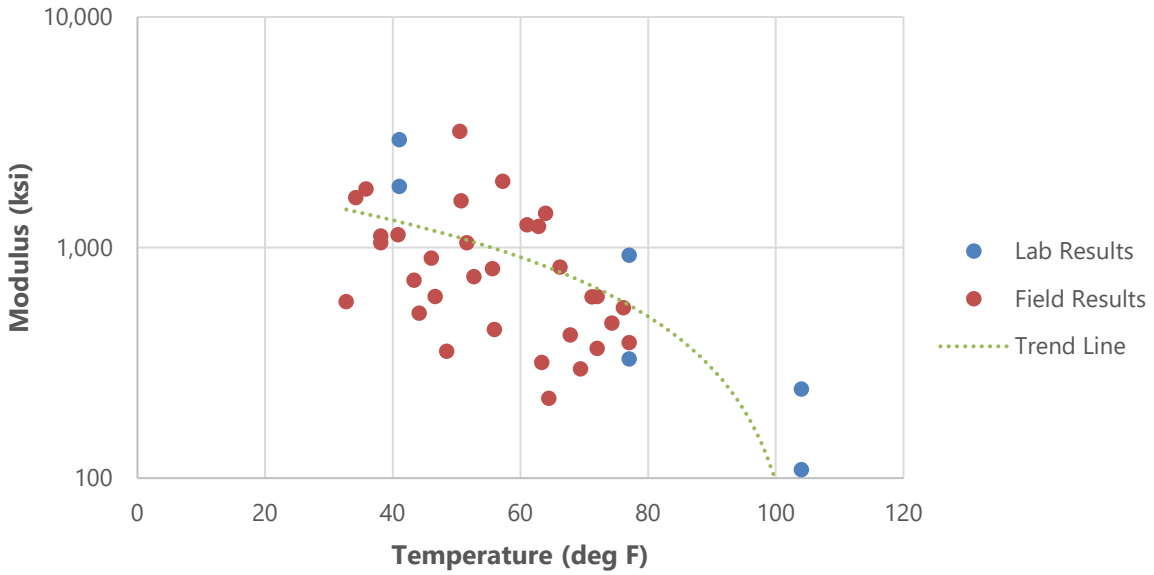

Figure 6. Field- and lab-derived AC resilient modulus values.

Deflection Regression Analyses

As an extension of the examination of the relationship between deflection, temperature and moisture content, a regression analysis was performed as part of the desktop study to statistically relate variations in deflection to the changes in both the referenced variables and the test section age. In this regression analysis, the age variable was calculated by subtracting the test date from the construction date (i.e., 6/1/1976). The mean was subtracted from the observed values for the temperature and moisture variables. The means of the temperature values and moisture values were equal to 66.13 °F and 8.53%, respectively. The position variable was defined as a categorical variable; its value was either 0 for the measurements obtained under the center of the load plate or 1 for the measurements captured at 48" from the load plate. Table 4 shows the outputs of the regression analysis. As shown, the regression coefficients for pavement temperature and moisture content are positive, which means that if either of these factors increases, the average pavement deflections will also increase. In addition, based on the computed p-values, it is apparent that the variation in the average deflection is highly correlated with changes in temperature, moisture content, and position, while the age of the section was not found to be significant.

Table 4. Regression analysis results

Factor	Regression Coefficient	P-value
Intercept	10.0328	< 2e-16
Age	-0.0002	0.2380
Temperature	0.0618	1.03e-15
Moisture	0.3526	8.85e-06
Position	-8.5905	< 2e-16
Temperature * Position	-0.0717	3.09e-13
Moisture * Position	-0.2659	0.00742

The effect of the temperature–position and moisture–position interactions on the deflections were also considered. The interaction between two factors is said to occur when the magnitude of the effect of one

factor on the dependent variable changes as the level of the other variable changes. Table 4 shows that these interaction effects are statistically significant and that they have a negative effect on the average pavement deflection. The impacts of these interactions are shown graphically in Figure 9 and Figure 10. As can be seen in Figure 9, when the AC temperature increases, average of pavement deflection at position 0 increases. However, when the AC temperature increases, average of pavement deflection at position 1 drops. Figure 10 shows that the effect of moisture content on deflection is significant for position 0, while it is less significant in position 1.

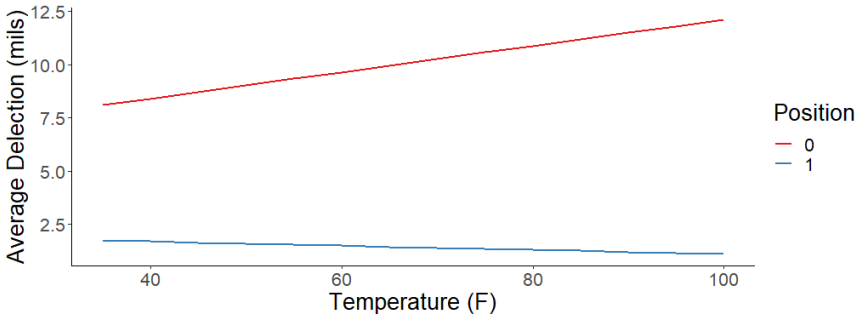

Figure 7. Interaction plot of temperature and position.

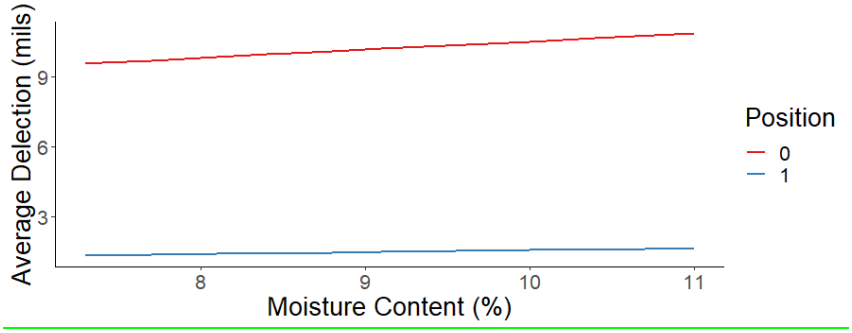

Figure 8. Interaction plot of temperature and position.

Ultimately, the regression analysis yielded the following model to predict pavement deflection (mils) based on pavement temperature (°F), subgrade moisture content (%), and measurement position (0 or 1):

$$Deflection = 10.02 + 0.06 * (Temperature - 66.13) + 0.37 * (Moisture\ Content - 8.53) - 8.59 * Position - 0.07 * (Temperature - 66.13) * Position - 0.27 * (Moisture - 8.53) * Position$$

At position 0 (under center of load plate), the above equation reduces to:

$$Deflection = 2.89 + 0.06 * Temperature + 0.37 * Moisture\ Content$$

While at position 1 (48 inches from center of load plate), the equation reduces to:

$$Deflection = 1.24 - 0.01 * Temperature + 0.10 * Moisture\ Content$$

The scatter plot of the predicted deflection values from the model versus the actual measured deflection values is shown in Figure 11. This plot shows a good correlation between measured and predicted deflection values with a coefficient of determination (R^2) of 0.99. The R^2 shows that 99% variability of deflection data can be explained by the variables in the model.

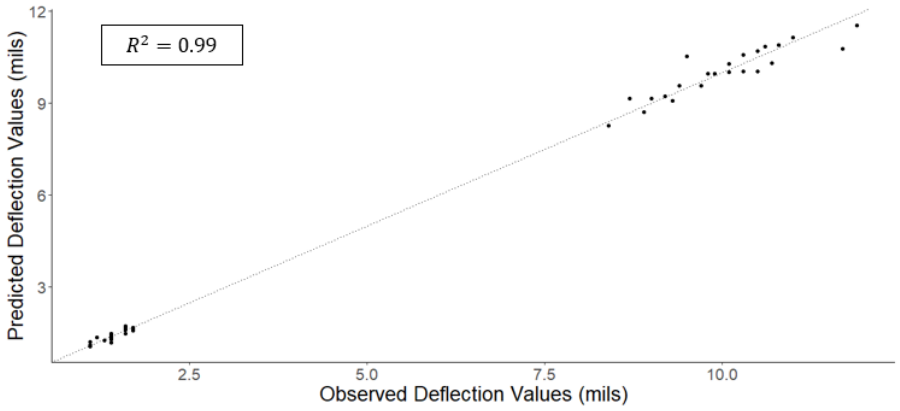

Figure 9. Predicted versus observed values of pavement deflection.

Climate History

The time history for average annual precipitation (from Modern-Era Retrospective analysis for Research and Applications or MERRA) since 1980 is shown in Figure 12. The mean precipitation recorded at the section was 49 inches for the period of analysis. Spikes in precipitation are observed in 1996, 2003, and 2009 when 63, 65, and 61 inches of precipitation were reported, respectively. The section is located near the Atlantic Ocean (approximately 10 miles away) and has been in the path of several hurricanes and tropical storms. Accordingly, the measured precipitation has likely played an important role in the overall performance of the test section.

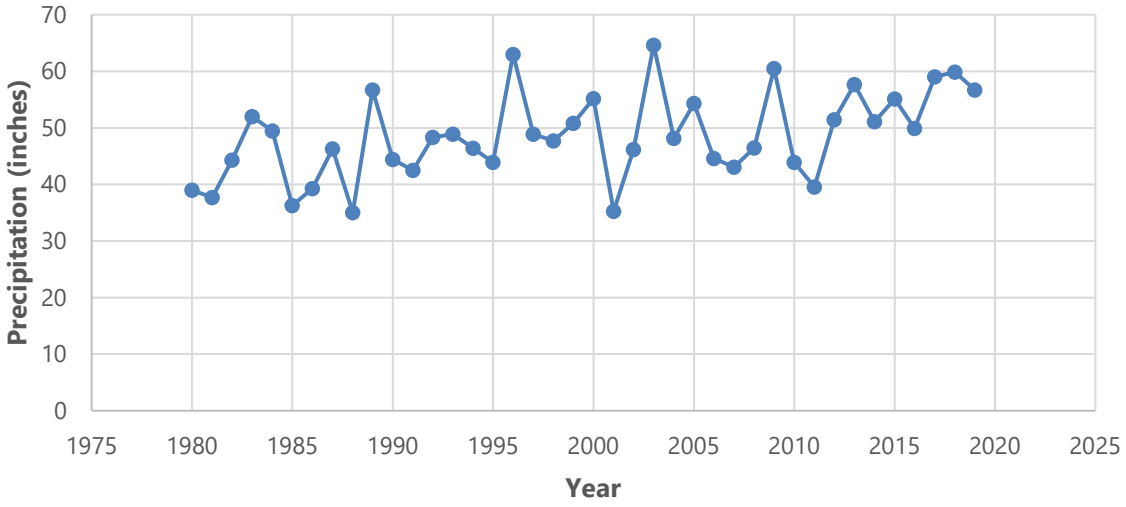

Figure 10. Average yearly precipitation over time.

Figure 13 shows the time history of the average annual freezing index (from MERRA) for the test site. The freezing index is the summation of the difference between freezing temperature and the average air temperature when it is less than freezing over a year's time. This index is an indicator of the harshness of the winter season relative to issues such as ground frost and low temperature cracking in pavements. As depicted in Figure 13, the freezing index values ranged from 1.8 deg F deg days (2002) to 174.6 deg F deg days (2015). Besides the spike in 2015, all freezing indices reported during the analysis period are well

below the 150 deg F deg days used to classify a freeze region. In turn, this indicates the freezing index is not likely a factor affecting the performance of the test section.

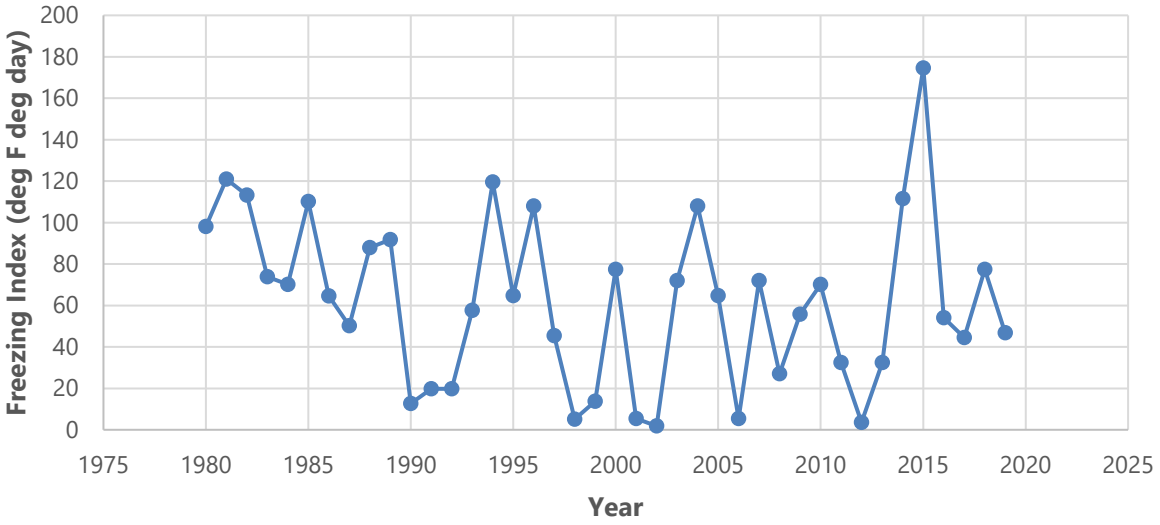

Figure 11. Average annual freezing index over time.

Truck Volume History

Figure 14 shows the annual average daily truck traffic (AADTT) data in the LTPP test lane by year. The annual truck traffic counts increase from 200 in 1976 to 345 in 2017, or approximately 4 additional trucks per day per year. The average number of ESALs reported on the section also increased over time as depicted in Figure 15. The number of ESALS increased from 31,827 in 1976 to 52,757 in 2017. The fluctuations in both the AADTT and ESALs reported for the test section are likely a result of the source of the data used over time. A combination of historical AADTT values, state provided AADTT values, monitored values (2000 and 2001), and values calculated using a linear growth function were used to report traffic along these test sections. The monitored data is based on counts collected over 20 days in 2000 and 146 days in 2001, indicating that the AADTT and ESALs calculated following 2001 are overreported.

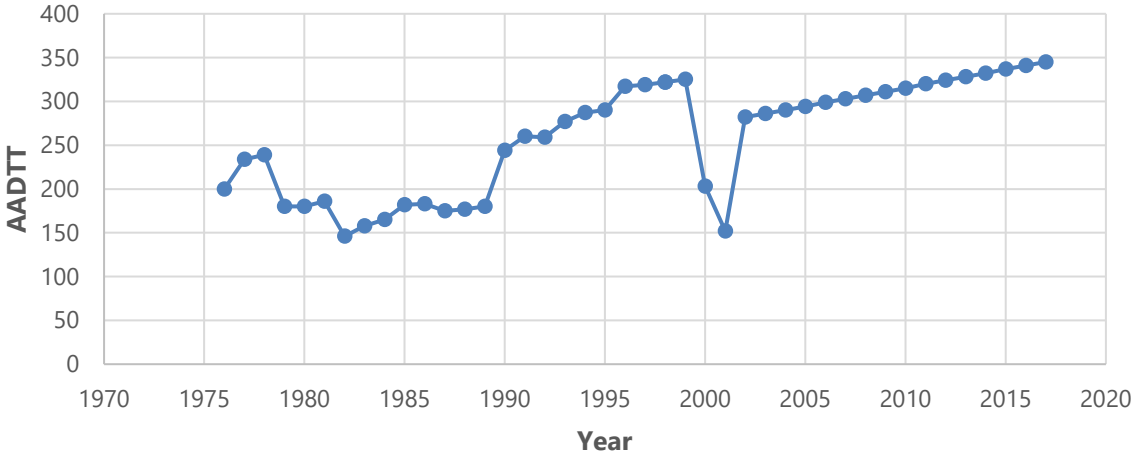

Figure 12. Average annual daily truck traffic (AADTT) history.

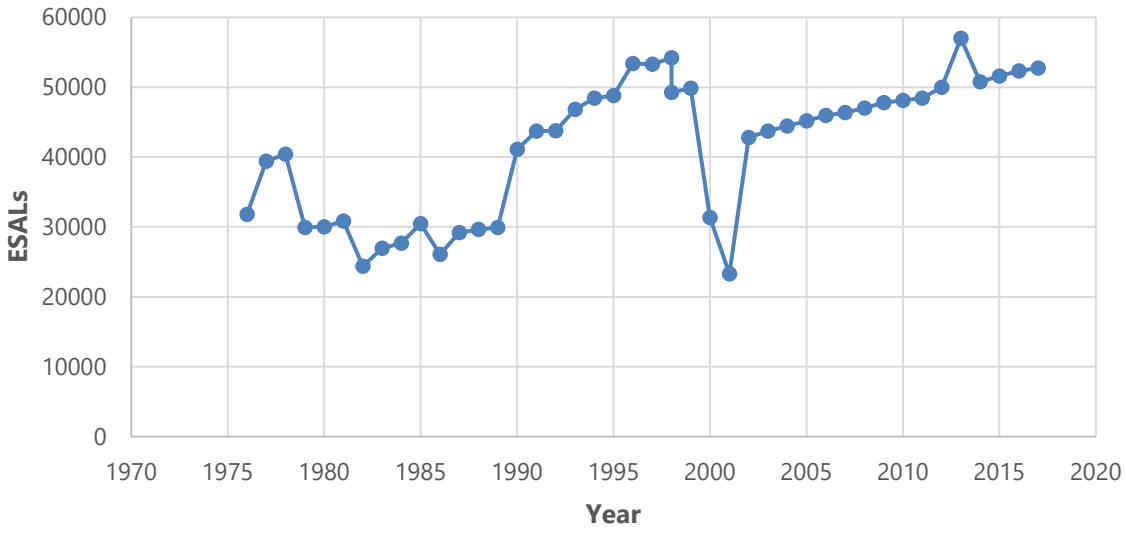

Figure 13. Estimated annual ESAL for vehicle classes 4-13 over time.

Pavement Distress History

The following summarizes the distresses observed on the test section, which was last monitored in 2016. Fatigue/alligator cracking, longitudinal cracking, transverse cracking, IRI, and rutting were assessed.

Fatigue/Alligator Cracking

Figure 16 shows the total area in which fatigue/alligator cracking was observed for the section between 1992 and 2016. While the graph obtained from InfoPave™ is labelled fatigue cracking, which implies a mechanism, the distress values reported includes both fatigue cracking (inside the wheelpath) and alligator cracking (outside the wheelpath).

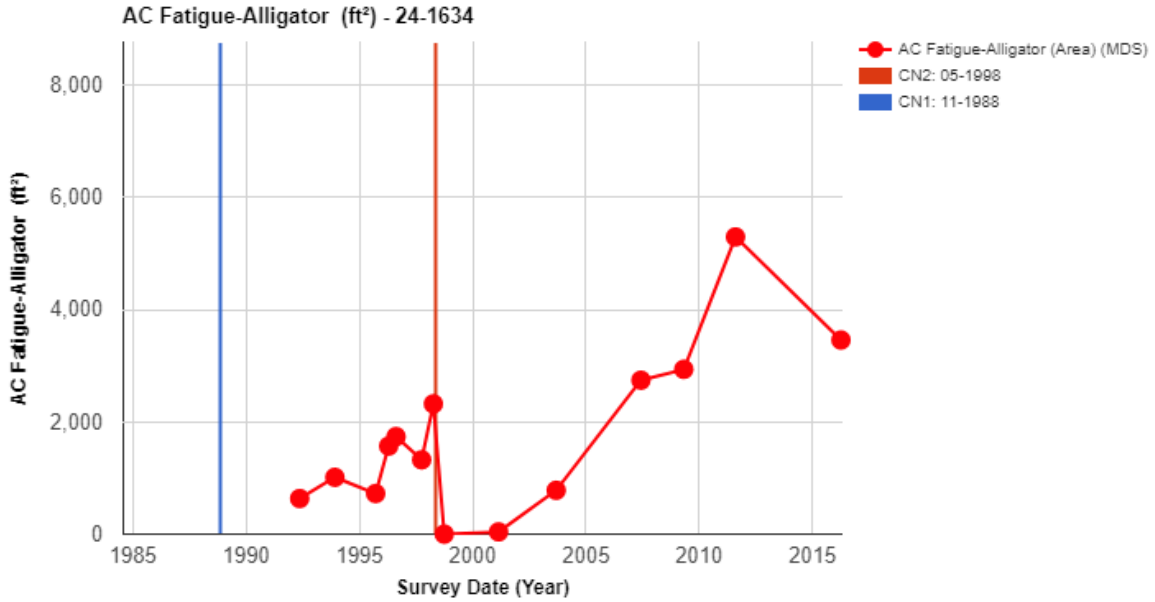

Figure 14. Time history of the length of fatigue cracking.

Fatigue/alligator cracking was first reported during the manual distress survey in 1992, when 634 ft^2 was observed. The fatigue/alligator cracking observed increased between 1992 and 1998, reaching 2,321 ft^2 prior to the overlay, propagating at a rate of 281 ft^2/year. After the overlay in May 1998, no fatigue cracking was observed until 2001 when 40 ft^2 of fatigue/alligator cracking was reported. Once observed, the cracking propagated at a rate of 525 ft^2/year between 2001 and 2011, or nearly double the rate of propagation prior to the overlay. The fatigue/alligator cracking observed in 2016 decreased to 3,457 ft^2, likely due to differences in rater opinions between the 2011 and 2016 surveys. The rater in 2011 considered the full area of the last 200 feet of the pavement section to be fatigue cracking, whereas the rater in 2016 did not. The fatigue cracking observed in 2016, shown in Figure 17, was predominantly located inside the wheel paths between 2 and 5 feet and 7 and 10 feet from the right edge of the lane.

Figure 15. Fatigue cracking on the section in 2011.

The increase in fatigue/alligator cracking following the overlay in 1998 may be related to pavement aging and overall structural degradation. The overlay event in 1998 did not appear to rejuvenate the original pavement structure and therefore, provided only near-term improvement. The original structure was constructed in 1976 and therefore, may had been experiencing increased cracking due to long-term environmental exposure and traffic loadings. This hypothesis is further supported by the high amounts of material degradation (raveling) reported throughout the section during the last two pavement distress surveys. Another potential reason for the increase in the fatigue/alligator cracking following the overlay in 1998 is the slightly increased levels of precipitation following the overlay. As water infiltrates the pavement layers, the base and subgrade tend to weaken (especially when reaching saturation conditions) possibly causing the increase in fatigue cracking observed.

Longitudinal Cracking

Non-wheel path (NWP) longitudinal cracking, depicted in Figure 18, was first reported during the manual distress survey in 1992, when 7 ft of cracking was observed. The NWP longitudinal cracking observed fluctuated between 1992 and 1998, with a spike in NWP longitudinal cracking in September 1995. The spike seemed to be related to the misidentification of fatigue cracking (outside the wheel path) as NWP longitudinal cracking. After the overlay in May 1998, no NWP longitudinal cracking was observed again until 2003 when 87 ft of NWP longitudinal cracking was observed. Once observed, the cracking

propagated at a rate of 101 ft/year between 2003 and 2016, reaching 1,403 ft in 2016. The NWP longitudinal cracking observed in 2016 was located in the center (between the wheelpaths) and at the edges of the lane as depicted in Figure 19. Moreover, the cracking observed following the overlay propagated more rapidly than prior to the overlay. It is hypothesized that the increase in NWP longitudinal cracking following the overlay is related to the increased levels of precipitation and aging/structural deterioration of the pavement section.

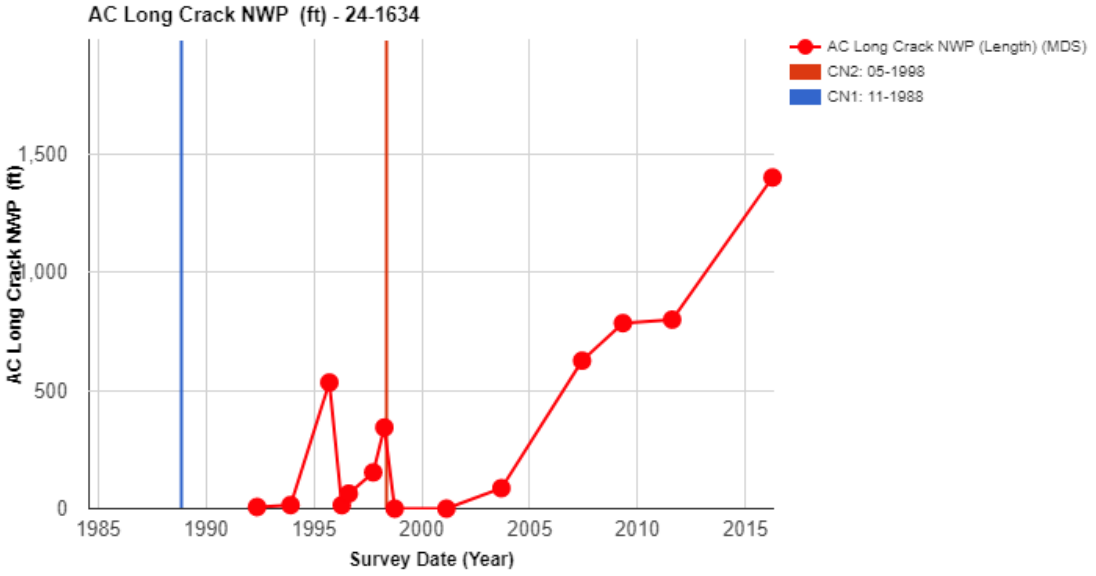

Figure 16. Time history of the length of NWP longitudinal cracks.

Figure 17. NWP longitudinal cracking on the pavement section in 2011.

The longitudinal cracking observed inside the wheel path (WP) was minimal throughout time. While some WP longitudinal cracking was observed both prior to and following the 1998 overlay, the maximum WP longitudinal cracking observed on the section was 51 feet in 2001. The longitudinal WP cracking that was reported was likely misidentified low-level fatigue/alligator-related cracking.

Transverse Cracking

Data on transverse cracking was collected between 1992 and 2016 as shown in Figure 20 and Figure 21. Unlike the fatigue/alligator cracking and NWP longitudinal cracking observed on the section, most of the transverse cracking observed occurred prior to the overlay in 1998. Transverse cracking was first reported during the manual distress survey in 1992, when 54 ft of cracking (27 cracks) was observed. The transverse cracking fluctuated between 1992 and 1997, reaching 225 ft (140 cracks) in 1997. However, the length of transverse cracks observed abruptly fell to 5 ft (1 crack) in April 1998, just prior to the AC overlay. The transverse cracking observed prior to this event consisted of short (1.5 ft), low severity cracks every 2 to 5 feet as shown in Figure 22. Given the typical length and severity, these cracks may have been difficult for raters to see and therefore, accurately report. After the overlay in May 1998, no transverse cracking was observed again until 2003 when 2 ft of transverse cracking (1 crack) was reported. Once observed, transverse cracking spiked in 2009 when 60 ft of cracking (40 cracks) was reported, and subsequently decreased reaching 10 ft (5 cracks) in 2016. This spike appeared to be the result of fatigue/alligator cracking being misidentified or reported as transverse cracking in 2009.

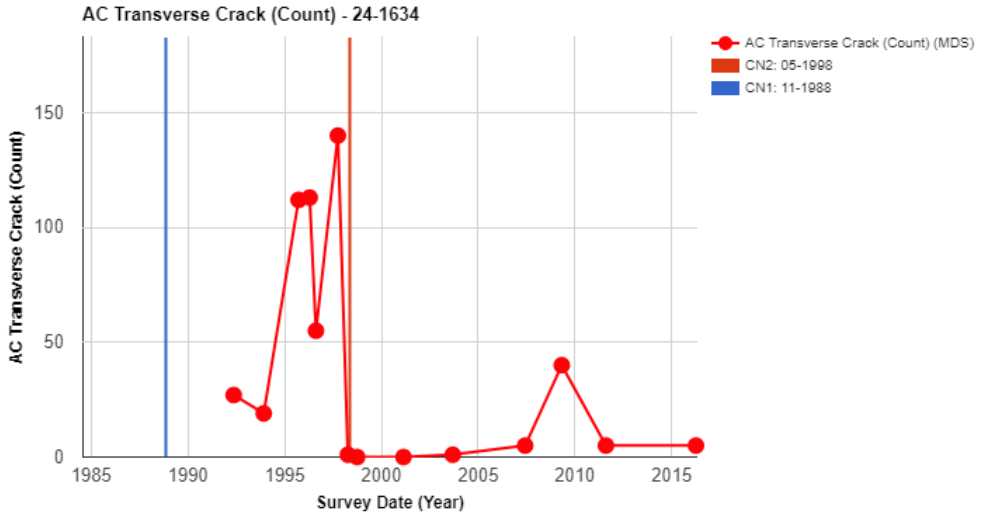

Figure 18. Time history of the number of transverse cracks.

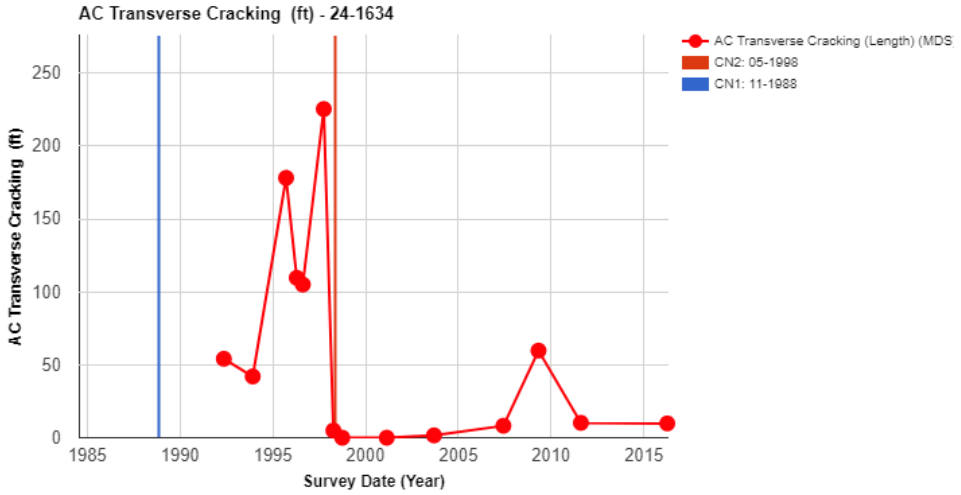

Figure 19. Time history of the length of transverse cracking.

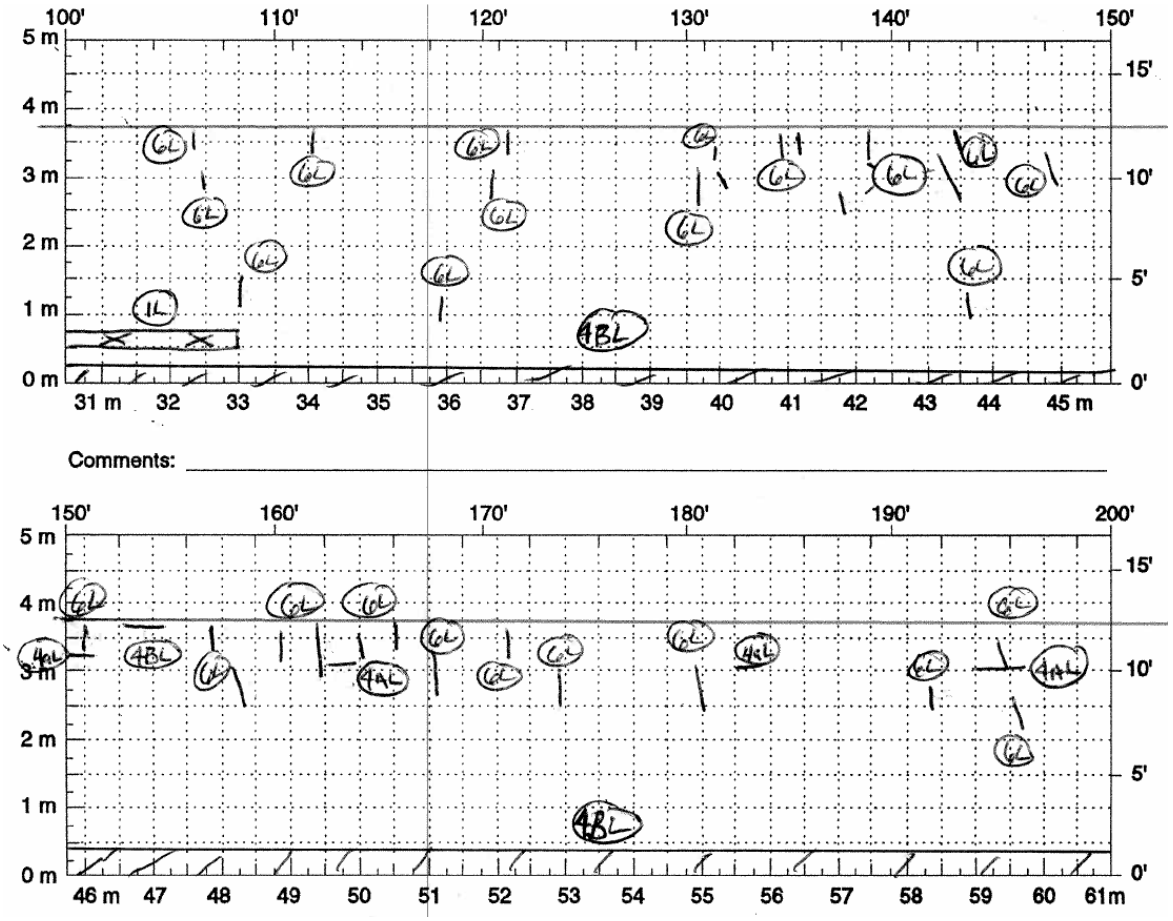

Figure 20. Transverse cracking reported on the pavement section in September 1995.

In addition to the findings presented above, it is important to note the presence of rumble strips along the centerline of the pavement section both prior to and following the overlay, which likely contributed to the transverse cracking reported throughout time. Prior to the overlay, a set of saw and seal lines, depicted in Figure 23, which are seen in the site images in 1993, were placed approximately every five feet. Following the overlay, conventional rumble strips were placed along the centerline throughout the length of the section. While per the LTPP Distress Identification Manual, these saw and seal areas should be counted as cracks, they are not reported as such in the distress surveys. Instead, transverse cracks that appear to be related to, but not including, these saw and seal lines are reported prior to the overlay.

Figure 21. Rumble strips prior to (left) and following (right) the 1998 overlay.

IRI

The average IRI measurements for the section over time are shown in Figure 24. The IRI on the section prior to the overlay averaged 60 in/mi, which means the performance of the pavement could be classified as "Good" based on FHWA performance definitions. Following the overlay of the pavement in 1998, the IRI dropped to 46 in/mi in July 1998. The IRI following the overlay remained low, with an average IRI of 48 in/mi between 1998 and 2016.

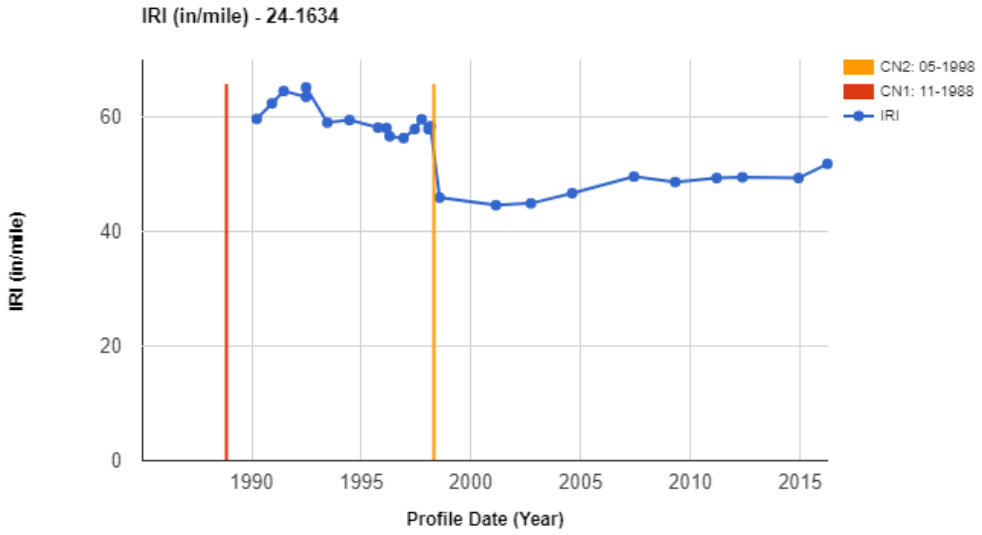

Figure 22. Time history plot of pavement roughness.

The low levels of IRI reported throughout the pavement's history do not align with amount of cracking observed on the section, particularly following the overlay when high amounts of fatigue/alligator cracking are observed. As depicted in the figure above, while IRI is relatively low throughout the section's history, higher IRI values are reported prior to the overlay and lower values are reported after the overlay. This observation points out why Departments of Transportation should not solely rely on IRI in assessing pavement performance. As the severity level of the cracking is predominantly low, the impacts on IRI are correspondingly low—higher severity cracking would likely result in increases in IRI, but probably not in a linear relationship.

Rutting

The average rut depths observed for the section over time are shown in Figure 25. The rutting on the section prior to the overlay ranged between 0.2 and 0.3 in, but oddly enough decreasing over time from 0.3 to 0.2 ins. Following the overlay in 1998, the average rut depth dropped to slightly over 0.1 in. However, the average rut depth then began to increase following the overlay, with values increasing to between 0.2 and 0.3 in between 1998 and 2016.

In addition to the average rut depth observed over time, the change in the transverse profile of the test section was also investigated. Using the transverse profiles of the test section at multiple locations, an analysis of the predominant layer in which plastic deformation occurs was assessed using the method developed in NCHRP 01-34a.[2] The NCHRP method, which was derived using finite element analyses of

[2] White, T., J. Haddock, A.J.T. Hand, & H. Fang. NCHRP 468: *Contributions of Pavement Structural Layers to Rutting of Hot Mix Asphalt Pavements*. National Cooperative Highway Program, Washington D.C., 2002.

rutting mechanisms in the HMA surface, base, and subgrade, is focused on the transverse profile characteristics indicative of permanent deformation such as densification, shear failure, or shear flow.

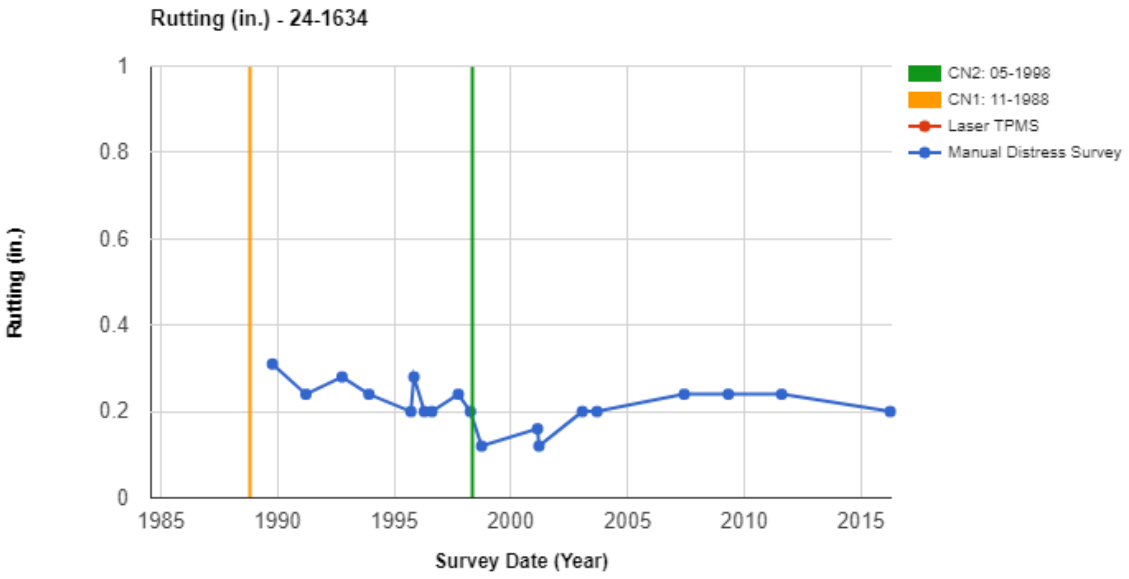

Figure 23. Time history plot of average rut depth.

The methodology consists of two key steps: calculation of distortion parameters and the use of criteria to classify the lowest layer in the pavement structure contributing to the ruts. Distortion parameters include the maximum rut depth (D), positive area, and negative area of a transverse profile. For each profile, the wire method is used to assess the maximum rut depth, which is the greatest perpendicular distance measured from the pavement surface to the wire reference line as depicted in Figure 26. Similarly, the positive area (A_P) and negative area (A_N) are the sum of the areas above and below the transverse profile reference line, respectively. Using these parameters, the ratio of positive area to negative area (R), total area (A_T), and the theoretical total areas for the HMA, base, and subgrade failure (C_1,C_2, and C_3, respectively) are calculated and used to assess the failed layer. The assessment of the parameters used to determine the lowest layer contributing to the pavement's surface deformation is described in Figure 27.

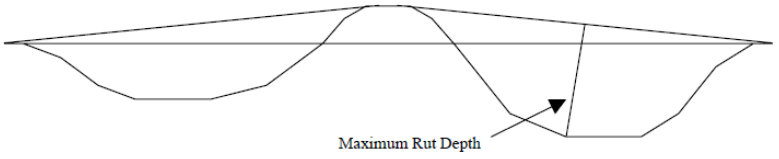

Figure A-1. Definition of maximum rut depth.

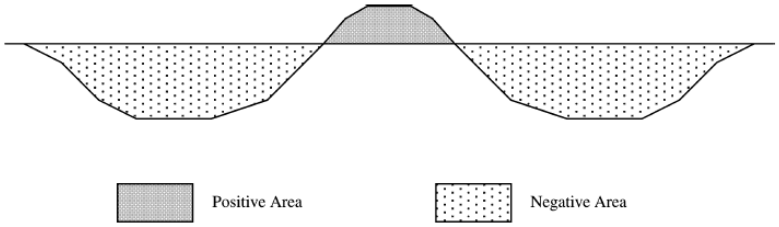

Figure 24. Transverse profile maximum rut depth and positive and negative areas (White et al., 2002)

Based on the analysis conducted for each of the transverse profiles of the test section (between 10 and 11 profiles spaced at 50 ft) for the 19 collection dates between October 1989 and April 2016, the predominant lowest layer contributing to rutting was calculated for each date of collection at multiple locations along the section. Table 5 summarizes the number of locations (or transverse profiles) along the test section where the layer most contributing to rutting was surface, base, and subgrade, respectively. As depicted in the table, the predominant layer contributing to rutting throughout time was the surface layer. However, following the AC overlay in 1998, some transverse profiles taken along the section showed the base layer as the lowest layer contributing to rutting. While a more in-depth assessment of this analysis cannot be pursued as the section has since been milled and overlaid, these findings can be used to support a potential rutting study proposed as a part of the Pooled Fund program. The study would focus on determining how the NCHRP method can be implemented for use within pavement management.

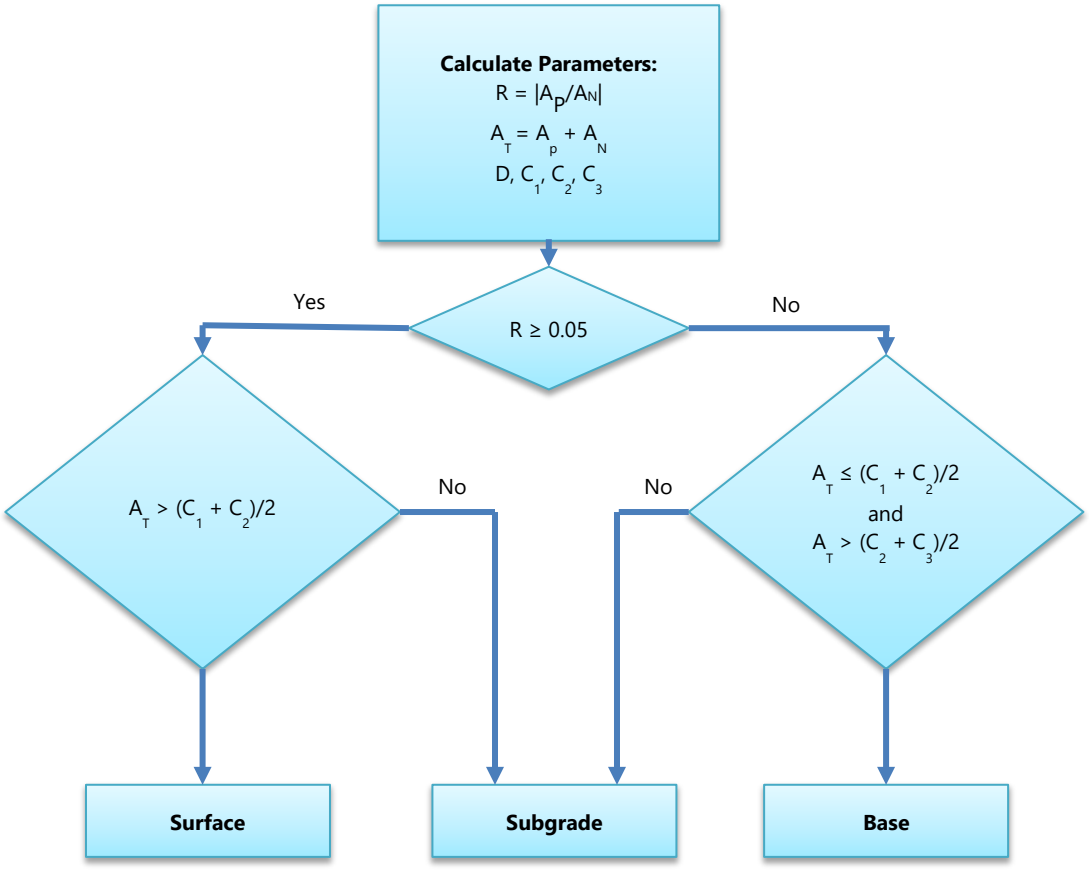

D= Maximum rut depth
A_p= Positive area (area above pavement surface line of a transverse profile)
A_n= Negative area (area below pavement surface line of a transverse profile)
C_1= (-858.21) D + 667.58, theoretical total area for HMA failure
C_2= (-1509) D -287.78, theoretical average total for base/subbase failure
C_3= (-2120.1) D – 407.95, theoretical average for subgrade failure

Figure 25. Failure layer determination using methodology by White et al. (2002)

Table 5. Lowest layer contributing to rutting

Date	Number of locations where rutting was related to the surface layer	Number of locations where rutting was related to the base layer	Number of locations where rutting was related to the subgrade layer
10/12/1989	10	-	-
03/21/1991	10	-	-
10/07/1992	9	-	1
12/02/1993	11	-	-
09/20/1995	11	-	-
11/06/1995	10	-	-
04/17/1996	11	-	-
08/14/1996	11	-	-
10/01/1997	11	-	-
04/08/1998	11	-	-
09/30/1998	11	-	-
02/22/2001	9	2	-
03/17/2001	10	1	-
01/24/2003	8	2	-
09/10/2003	10	1	-
06/07/2007	10	1	-
04/28/2009	9	2	-
08/10/2011	10	1	-
04/05/2016	8	3	-

SUMMARY OF FINDINGS

LTPP test section 24_1634 is located on State Route 90, eastbound, in Worcester County, Maryland. State Route 90 is a rural principal arterial with one lane in the direction of traffic. The test section is classified as being in a Wet, No-Freeze climate zone. The test section was constructed in 1976 and was accepted into

the LTPP Program as part of the GPS-2 experiment in November 1988. The pavement structure at the time of its incorporation into the LTPP program consisted of 3.5 inches of asphalt concrete (AC), 4.8 inches of bound (sand asphalt) treated base, and 13 inches of unbound granular subbase over a fine-grained subgrade layer. The next construction event occurred in May 1998, when the test section received shoulder restoration and 3.2-inch AC overlay. Subsequently, the test section was moved to the GPS-6C AC Overlay Using Modified Asphalt of AC Pavement-No Milling study. While no additional construction events were reported following 1998, the test section was found to be milled and overlaid sometime after the last survey date in 2016 (the specific year of the event is still being determined), and therefore, the site is now considered Out of Study (OOS).

The memorandum was focused on the following:

1. **Examining the reason(s) for high amounts of fatigue and NWP longitudinal cracking following the AC overlay of the test section**. The increase in fatigue/alligator and NWP longitudinal cracking following the overlay in 1998 seems to be related to pavement aging and overall structural degradation. The overlay event in 1998 did not appear to rejuvenate the original pavement structure and therefore, provided only near-term improvement. The original structure was constructed in 1976 and therefore, may had been experiencing increased cracking due to long-term environmental exposure and traffic loading. This hypothesis is further supported by the high amounts of material degradation (raveling) reported throughout the section during the last two pavement distress surveys. Another potential reason for the increase in the cracking following the overlay in 1998 is the slightly increased levels of precipitation following the overlay. As water infiltrates the pavement layers, the base and subgrade tend to weaken (especially when reaching saturation conditions) causing the increase in fatigue cracking observed.
2. **Examining the reason(s) for the extremely low IRI on the pavement section despite the presence of cracking throughout time**. The low levels of IRI reported throughout the pavement's history do not align with amount of cracking observed on the section, particularly following the overlay when high amounts of fatigue/alligator cracking were observed. This observation highlights why Departments of Transportation should not solely rely on IRI in assessing pavement performance. As the severity level of the cracking is predominantly low, the impacts on IRI are correspondingly low—higher severity cracking would undoubtedly result in increases in IRI, but probably not in a linear relationship.
3. **Examining the relationship between the pavement deflection, pavement temperature, and subgrade moisture content using the SMP dataset.** In this study, the average deflection observed over time when it was monitored under the SMP was reviewed to associate deflections with climate changes related to seasonal temperature and moisture fluctuations. The change in deflection under the load plate over time appeared to be directly related to the change in pavement temperature over time. For the most part, increases and decreases in pavement temperature corresponded to increases and decreases in the average deflections. However, the relationship between the average deflection under the load plate and moisture content of the test section was less clear. The change in deflection 48 inches from the load plate (Sensor 7) appeared to be related to the change in moisture content over time, but not to the change in subgrade temperature over time. Moreover, a regression to predict deflections as a function of pavement temperature, moisture content and FWD sensor location was successfully developed.

FORENSIC EVALUATION RECOMMENDATIONS

While the test section was reported as active when it was initially nominated for investigation, as noted earlier, this test section was found to have been milled and overlaid when preparing to schedule the field evaluation. For this reason, no follow-up field investigations are recommended for this test section.